PHYSICAL REVIEW B **66**, 235405 (2002)

Nature of lattice distortion in one-dimensional dangling-bond wires on Si and C

Jun-Hyung Cho and Leonard Kleinman
Department of Physics, University of Texas, Austin, Texas 78712-1081

(Received 1 October 2002; published 13 December 2002)

The structure of one-dimensional ‘‘dangling-bond wires’’ fabricated on H-passivated Si and diamond (001) surfaces has been determined by first-principles calculations. The dangling-bond wire on Si(001) exhibits a lattice distortion with an alternating up and down displacement, whereas such a distortion is suppressed in that on C(001). These contrasting behaviors for both cases are attributed to the different chemical trend of Si and C dangling bonds in a rehybridization of the dangling orbital. Our analysis shows that the underlying mechanism of the lattice distortion in the dangling-bond wire on Si(001) is not related with a Peierls instability, but is analogous to that of the dimer reconstruction at the clean Si(001) surface.

DOI: 10.1103/PhysRevB.66.235405 PACS number(s): 68.35.Bs, 73.20.At, 73.22.−f

Recently, the scanning tunneling microscope (STM) has been used to manipulate single atoms on surfaces including lateral movement and vertical transfer,[1] and therefore it becomes a unique tool capable of fabricating atomic-scale structures as well as imaging surface structures. An important example of such fabrication of nanostructures is the dangling-bond (DB) wire[2] which can be produced by the selective removal of hydrogen atoms from an H-passivated Si(001) surface along the Si dimer row [see Fig. 1(a)]. This DB wire has a single dangling bond per Si atom, offering a one-dimensional (1D) metallic system with a half-filled surface state in the energy gap. Thus, a Peierls instability of the 1D metal is expected to drive a metal-insulator transition, accompanying a charge-density wave and a lattice distortion with a doubled periodicity.

In their density-functional theory (DFT) calculation for the DB wire on an H-passivated Si(001) surface, Watanabe *et al.*[3] predicted the presence of the Peierls instability that accompanies a metal-insulator transition and a lattice distortion. A recent STM study by Hitosugi *et al.*[4] observed an alternating vertical displacement (i.e., up and down) of the surface Si atoms composing the DB wire on Si(001). Based on the experimental observations and DFT calculations of several DB wires with different lengths, Hitosugi *et al.* claimed that the observed lattice distortion can be described by a Jahn-Teller distortion, with charge redistribution along the DB wire (i.e., almost a unit charge transfer from the down Si atom to the up Si atom) and pairing of the second-layer Si atoms. Thus, the lattice distortion in the DB wire on Si(001) was explained by the different mechanisms, i.e., the Peierls[3] and the Jahn-Teller[4] distortion for the infinite- and the finite-length wire, respectively.

In this paper, we present a DFT calculation for the DB wire on H-passivated Si(001) using the generalized-gradient approximation (GGA). Note that all previous DFT calculations[3–5] were performed within the local-density approximation (LDA). In order to shed light on the origin of the lattice distortion observed in the DB wire on Si(001), we also investigate the structural and electronic properties of the DB wires on H-passivated C(001). Such an additional study will stimulate the fabrication of atomic-scale structures on C(001), which is of particular technological importance related with diamond thin film growth. On Si(001) a lattice distortion is found to be pronounced with a height difference of 0.74 Å between the up and down Si atoms in the DB wire [see Fig. 1(b)], accompanying the metal-insulator transition with a band gap of greater than 0.36 eV. On the other hand, the DB wire on C(001) in which a half-filled surface state is present with a nested segment of the Fermi surface does not show a Peierls instability with lattice distortion. Therefore

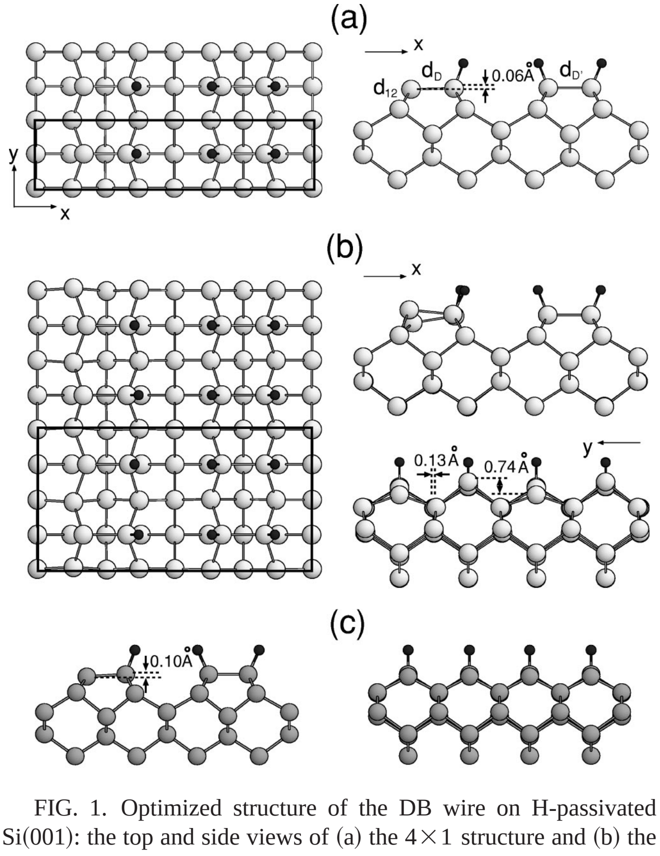

FIG. 1. Optimized structure of the DB wire on H-passivated Si(001): the top and side views of (a) the 4×1 structure and (b) the 4×2 structure. For the DB wire on H-passivated C(001) the two side views are given in (c). The large and small circles represent Si (or C) and H atoms, respectively. The rectangles in the top views of (a) and (b) represent the 4×1 and 4×2 unit cells, respectively. The *x* and *y* directions are $[1\bar{1}0]$ and [110], respectively.

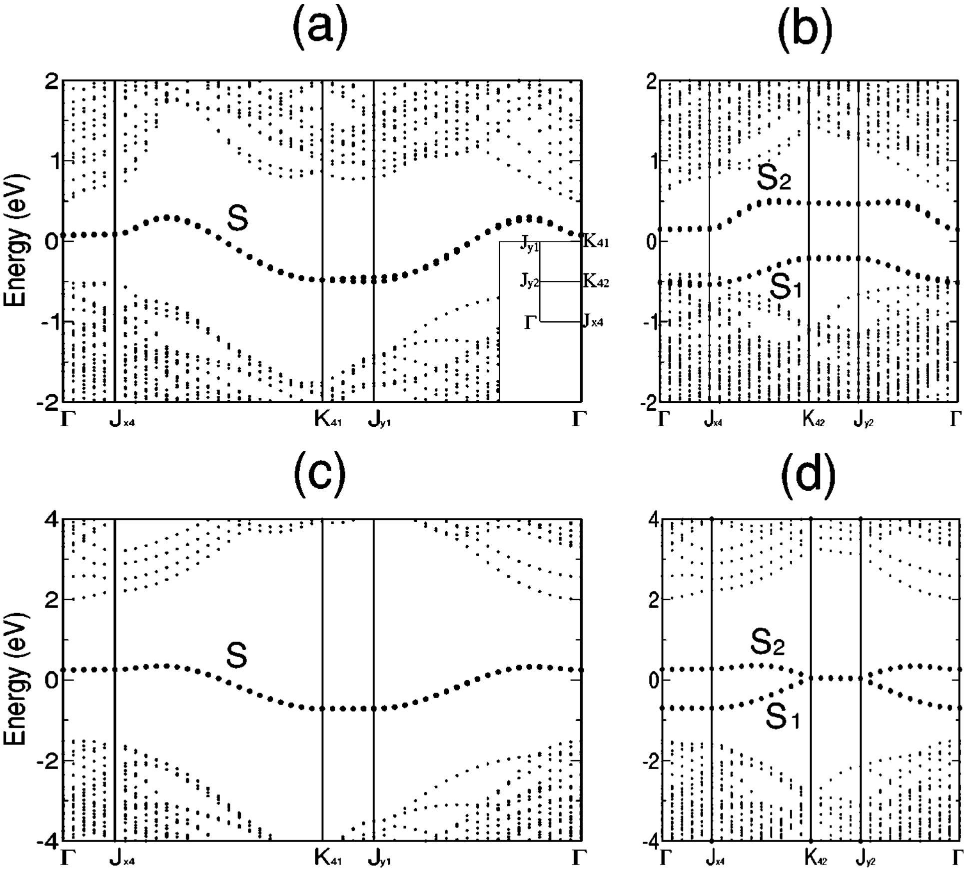

FIG. 2. Surface band structure of the DB wire on H-passivated Si(001): (a) the 4×1 structure and (b) the 4×2 structure. The corresponding ones for the DB wire on H-passivated C(001) are given in (c) and (d). The inset in (a) shows the surface Brillouin zone of the 4×1 unit cell. The large circles represent the surface state S (S_1 and S_2) of the 4×1 (4×2) DB structure and the small circles represent the eigenvalues obtained from the slab calculations. A doublet of surface states is associated with the two different sides of the slab.

the DB wire on C(001) is metallic, contrasting with the nonmetallic DB wire on Si(001). In the DB wire on Si(001) the up (down) Si atom approaches sp^3(sp^2)-like hybridization, accompanied by charge transfer. Here, the charge transfer involves only the Si dimer bond and the two back bonds (not the adjacent dangling bonds). This alternating up and down distortion is energetically favored as a consequence of the reduced repulsive Coulomb interaction between rehybridized dangling bonds. Thus, the nature of the lattice distortion in the DB wire on Si(001) is analogous to the alternating buckled dimer reconstruction at the clean Si(001) surface, rather than a Peierls distortion or a Jahn-Teller distortion causing the charge transfer between dangling bonds.

The total-energy and force calculations were carried out using density-functional theory[6] within the generalized-gradient approximation.[7] The Si (C) and H atom are described by norm-conserving[8] (ultrasoft[9]) pseudopotentials. A periodic slab geometry was employed with 12 atomic layers and passivated H atoms on both sides of the slab. The vacuum spacing between these slabs is about 10 Å. A plane-wave basis set was used with a 15- and 25-Ry cutoff for Si(001) and C(001), respectively. The **k** space integration was done with 16 and 8 points in the surface Brillouin zone of the 4×1 and 4×2 unit cells, respectively. All atoms except the two central planes were allowed to relax along the calculated Hellmann-Feynman forces until all the residual force components were less than 1 mRy/bohr.

We first study the structure of the DB wire on an H-passivated Si(001) surface. Here, we consider an infinite-length wire by employing the 4×1 unit cell where the lines of the single dangling bond are separated, perpendicular to the Si dimer row, by an additional H-passivated Si dimer row. The optimized structure is shown in Fig. 1(a). We find that the position of the surface Si atom composing the DB wire is lowered by 0.06 Å compared to that of the H-bonded Si atom. Our band-structure calculation for the 4×1 DB wire shows that the surface state S crosses the Fermi level at almost the midpoints of the symmetry lines of $J_{x4}K_{41}$ and ΓJ_{y1} [See Fig. 2(a)]. This crossing of the S state is found to show no dispersion along the $J_{y2}K_{42}$ line. It is expected that a charge-density wave coupled to a lattice vibration of wavelength $2a_y$ along the Si dimer row might lead to a Peierls-like instability. To examine this possibility, we performed an optimization of the symmetry-unrestricted geometry with a doubled periodicity using the 4×2 unit cell. Our optimized structure for the 4×2 DB wire is shown in Fig. 1(b). The surface Si atoms composing the DB wire are displaced up and down alternatively, yielding a height difference of 0.74 Å between the up and down atoms. As a consequence of this vertical relaxation of the surface Si atoms, the second-layer Si atoms bonding to the up atom move equally toward each other by 0.13 Å [see Fig. 1(b)]. This distorted 4×2 structure is found to be more stable than the 4×1 structure by 43 meV per 4×1 unit cell. The total energy gain results from the electronic contribution due to a band gap opening at the Fermi level [see Fig. 2(b)]. We find the direct band gap of 0.69 (0.68) eV at the K_{42} (J_{y2}) point and the indirect one of 0.36 eV between K_{42} and Γ.

There are somewhat large differences between theoretical calculations[3–5] for the structural, electronic, and energetic

TABLE I. Calculated height difference $\Delta d_{\text{up-dn}}$ (Å) between the up and down atoms, band gap ΔE_{gap} (eV), and energy gain ΔE(meV) for the 4×2 DB structure on H-passivated Si(001), in comparison with previous theoretical results. For ΔE_{gap} the direct and indirect (in parenthesis) band gaps are given together. The data of Hitosugi *et al.* are for the DB wire containing three dangling bonds, whereas ΔE in parenthesis represents the value of an infinite-length DB wire.

	$\Delta d_{\text{up-dn}}$	ΔE_{gap}	ΔE
Watanabe *et al.*[a] (LDA)	0.16	0.126 (0.025)	7
Hitosugi *et al.*[b] (LDA)	0.50		47 (54)
Bowler and Fisher[c] (LDA)	0.67		105
This work (GGA)	0.74	0.68 (0.36)	43

[a] Reference 3.

[b] Reference 4.

[c] Reference 5.

properties of the DB wire on Si(001). The LDA calculation carried out by Watanabe *et al.*[3] gives too small height difference between the up and down atoms ($\Delta d_{\text{up-dn}} = 0.16$ Å) and a band gap ($\Delta E_{\text{gap}} = 0.126$ and 0.025 eV) and an energy gain ($\Delta E = 7$ meV/DB) due to the lattice distortion (see Table I). This underestimation compared to other calculations[4,5] may be due to the use of less **k** points, i.e., only four (two) **k** points in the surface Brillouin zone of the 4×1 (4×2) unit cell. The three other calculations including the present one give similar values for $\Delta d_{\text{up-dn}}$ ranging from 0.50 to 0.74 Å, but the LDA calculation of Bowler and Fisher[5] gives too large an energy gain ($\Delta E = 105$ meV/DB) compared to the LDA result (54 meV/DB) of Hitosugi *et al.*[4] and the present GGA result (43 meV/DB).

In Fig. 3, we plot the charge density of the surface states S_1 and S_2 [displayed in Fig. 2(b)] at the J_{y2} point. The corresponding charge density plots at the K_{42} point are almost identical with those at J_{y2}. The charge character of the occupied S_1 (unoccupied S_2) state reveals dangling bonds, which are localized at the up (down) Si atoms. Previous theoretical studies,[3–5] therefore, concluded that a unit charge of the dangling bond in the down atom is totally transferred to the up atom. We need to caution that the different charge characters of the S_1 and S_2 states cannot be regarded as the whole charge transfer from the down to the up atom.

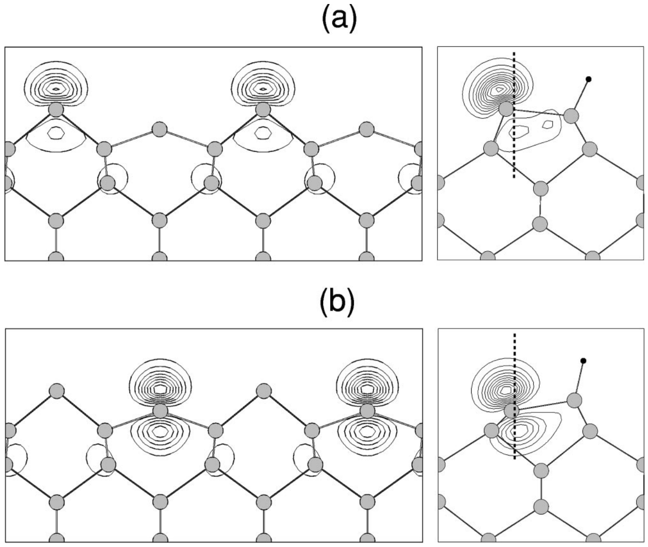

FIG. 3. Charge characters of (a) the occupied (S_1) and (b) the unoccupied (S_2) surface state of the 4×2 DB structure on H-passivated Si(001). The charge densities are obtained at the J_{y2} point. The first contour line is at 0.001 e/bohr^3 with spacings of 0.001 e/bohr^3. In (a) and (b) the left-side plot is drawn in the vertical yz plane indicated as the dotted line in the right-side plot.

In order to examine the charge redistribution occurring in the DB wire on Si(001), we calculate the valence charge density for the 4×1 and 4×2 DB structures. Compared to the 4×1 result [Fig. 4(a)], the charge densities in the 4×2 [Figs. 4(b) and 4(c)] clearly show that the charge of the Si dimer bond when the dangling bond Si atom is up (down) atom is depleted (accumulated). This accumulation (depletion) is accompanied by a depletion (accumulation) from (at) the upper region of the atom. As a result, the Si dimer-bond length involving the up (down) atom increases (decreases) to $d_D = 2.46$ (2.39) Å, compared to 2.41 Å in the 4×1 DB structure (see Table II). Note that the back bonds of the up (down) atom show the same trend by increasing (decreasing) the bond length as $d_{12} = 2.40$ (2.32) Å, compared to 2.34 Å in the 4×1 DB structure. Thus, it is likely that the Si dimer bond and the two back bonds connecting to the up (down) atom contribute to charge accumulation (depletion) in the upper region of the up (down) atom, leading to the bond reordering of sp^3(sp^2)-like hybridization. We can have more information about the charge redistribution in the DB wire by comparing the charge densities [Figs. 4(b) and 4(c)] of the 4×2 DB structure with that [Fig. 4(d)] of the clean Si(001)-2×2 surface, where dimer structures are alternatively buckled along the dimer row. We see that the contours around the up and down atoms in the DB wire are quantitatively similar to those at the clean Si(001) surface and that the ionic H-Si bond is formed by pulling electrons from the H-bonded Si atom. The diminution of Si charge due to the formation of the Si-H bond is seen along the Si dimer bond in Fig. 4(b) where the 0.08-e/bohr^3 contour, present for the clean surface [see Fig. 4(d)], is missing. Such diminution weakens in Fig. 4(c), where H is bonded to the up atom of the Si dimer, because the larger charge of the up atom due to dimer buckling takes part in the formation of the Si-H bond. Note that our calculated energy difference between the 2×1 and 2×2 structures of the clean Si(001) surface is 85 meV/dimer. Considering that the DB wire is obtained by H passivation on one side of Si dimers, this energy gain exactly corresponds to that due to the lattice distortion in the DB wire ($\Delta E = 43$ meV/DB). Thus, the nature of the lattice distortion in the DB wire on Si(001) is similar in charge density and energy to that of the alternating buckled dimer reconstruction at the clean Si(001) surface.

Next, we present our results for the atomic and electronic structures of the DB wire on an H-passivated C(001) surface. The optimized structure for the 4×1 DB structure is shown in Fig. 1(c). Similar to the case on Si(001), the position of the surface C atoms composing the DB wire is lowered by

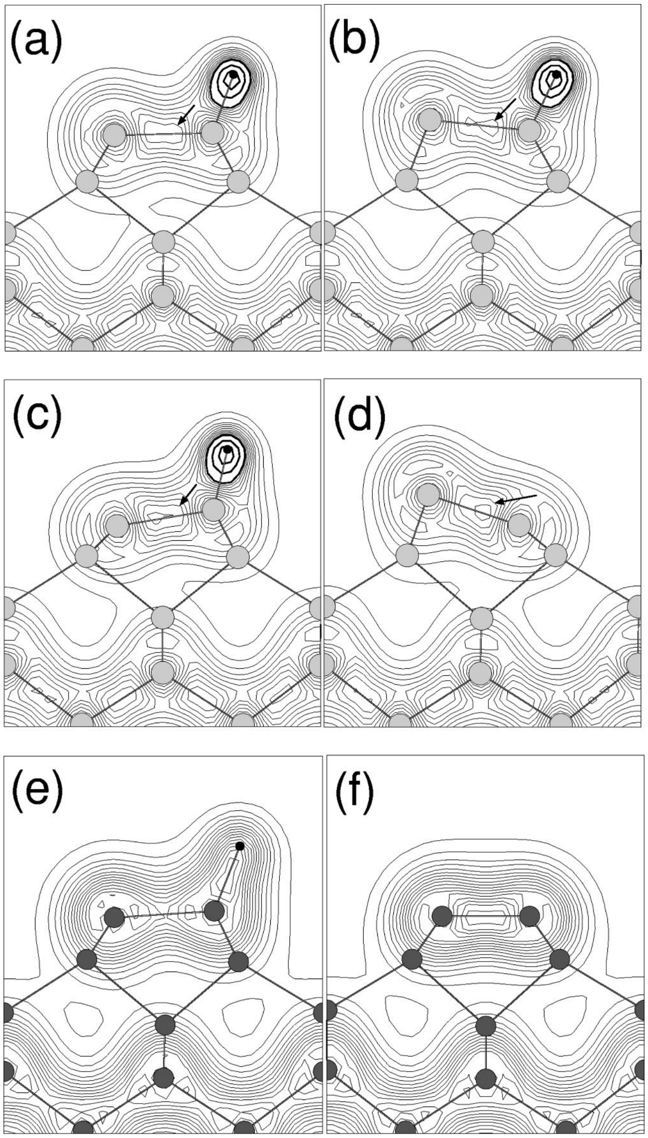

FIG. 4. Contour plots of the valence charge density for various structures: (a) the 4×1 DB structure on H-passivated Si(001), (b) and (c) the 4×2 DB structure on H-passivated Si(001), (d) the Si(001)−2×2 surface, (e) the 4×1 DB structure on H-passivated C(001), and (f) the C(001)-2×1 surface. The two different cuts through the up and down atoms are given in (b) and (c), respectively. Two kinds of contour spacings in (a), (b), and (c) are used. The first thin line is at 0.008 e/bohr^3 with spacings of 0.008 e/bohr^3. The first thick line is at 0.088 e/bohr^3 with a spacing of 0.04 between thick lines. In (d) the first contour line is at 0.008 e/bohr^3 with spacings of 0.008 e/bohr^3. In (e) and (f) the first contour line is at 0.018 e/bohr^3 with spacings of 0.018 e/bohr^3. The arrows in (a), (b), (c), and (d) represent the contour line of 0.072 e/bohr^3.

0.10 Å compared to that of the H-bonded C atom. The Fermi surface of this structure has a nested vector $2k_F = \pi/a_y$ Å^{-1} (a_y=2.526 Å), as the Fermi-level crossing of the S state occurs at the midpoints of the symmetry lines $J_{x4}K_{41}$ and ΓJ_{y1} [see Fig. 2(c)]. Thus, a Peierls instability might be expected, but we cannot find any lattice distortion within a 4×2 periodicity and therefore the obtained surface band structure [Fig. 2(d)] does not show a metal-insulator transition with the band gap at the Fermi level. The charge density plot [Fig. 4(e)] of the DB wire on C(001) shows a large difference along the C dimer, compared to that [Fig. 4(f)] of the clean C(001)-2×1 surface. In the latter a maximum of the huge charge accumulation exists in the center of the C dimer with a magnitude of greater than 0.306 e/bohr^3, whereas in the former such accumulated charge of a strong double bond disappears by the formation of the C-H bond. As a result, the C dimer-bond length in the DB wire increases as d_D=1.59 Å, compared to 1.39 Å in C(001)-2×1 (see Table II). Despite this weakened bonding of C dimer in the DB wire the lattice distortion accompanied by charge transfer does not occur.

TABLE II. Calculated bond lengths for the DB wires and the clean surfaces. For the definitions of d_D, d_{12}, and $d_{\mathrm{D}'}$ see Fig. 1(a). The data in parentheses represent the bond lengths associated with the down atom.

	d_D	d_{12}	$d_{\mathrm{D}'}$
4×1-DB/Si(001)	2.41	2.34	2.42
4×2-DB/Si(001)	2.46 (2.39)	2.40 (2.32)	2.42
Si(001)-2×2	2.36	2.40 (2.35)	
4×1-DB/C(001)	1.59	1.49	1.62
C(001)-2×1	1.39	1.51	

The absence of lattice distortion in the DB wire on C(001) indicates that the charge redistribution which produces the bond reordering of dangling bonds is not so favorable as the case of the DB wire on Si(001). This contrasting behavior in the charge redistribution can be traced to the strong C-C bonding, caused by more localized C 2p orbitals due to the absence of core p orbitals. The electronic energy gain obtained by charge redistribution cannot prevail over the larger elastic energy cost of a lattice distortion on the C(001) DB wire. In this sense, the DB wire on H-passivated C(001) involves the same structural propensity as the clean C(001) surface, where a symmetric dimer reconstruction with a 2×1 unit cell is favored.

In conclusion, our comparative theoretical studies for the DB wires on Si(001) and C(001) clarify the underlying mechanism of the lattice distortion observed in the former. The origin of the lattice distortion in the DB wire on Si(100) is a strong bond reordering of dangling orbitals by charge redistribution, therefore diminishing repulsive interaction between the dangling bonds.[10,11] Our results do not support previous proposed mechanisms such as a Peierls distortion and a Jahn-Teller distortion accompanying the charge transfer between dangling bonds. Finally, we wish to emphasize that the DB wire on C(001) is one of the few cases of a *conducting* atomic wire on an insulator.

This work was supported by the National Science Foundation under Grant No. DMR-0073546, the Welch Foundation (Houston, Texas), National Partnership for Advanced Computational Infrastructure at UC San Diego, and the Advanced Computing Center for Engineering and Science (The University of Texas at Austin).

[1] *Atomic and Nanometer Scale Modification of Materials: Fundamentals and Applications*, edited by Ph. Avouris (Kluwer Academic, Dordrecht, The Netherlands, 1993).

[2] J.W. Lyding, T.-C. Shen, J.S. Hubacek, J.R. Tucker, and G.C. Abeln, Appl. Phys. Lett. **64**, 2010 (1994).

[3] S. Watanabe, Y.A. Ono, T. Hashizume, and Y. Wada, Phys. Rev. B **54**, R17 308 (1996); Surf. Sci. **386**, 340 (1997).

[4] T. Hitosugi, S. Heike, T. Onogi, T. Hashizume, S. Watanabe, Z.-Q. Li, K. Ohno, Y. Kawazoe, T. Hasegawa, and K. Kitazawa, Phys. Rev. Lett. **82**, 4034 (1999).

[5] D.R. Bowler and A.J. Fisher, Phys. Rev. B **63**, 035310 (2000).

[6] P. Hohenberg and W. Kohn, Phys. Rev. **136**, B864 (1964); W. Kohn and L.J. Sham, Phys. Rev. **140**, A1133 (1965).

[7] J.P. Perdew, K. Burke, and M. Ernzerhof, Phys. Rev. Lett. **77**, 3865 (1996).

[8] N. Troullier and J.L. Martins, Phys. Rev. B **43**, 1993 (1991).

[9] D. Vanderbilt, Phys. Rev. B **41**, 7892 (1990); K. Laasonen, A. Pasquarello, R. Car, C. Lee, and D. Vanderbilt, *ibid.* **47**, 10 142 (1993).

[10] C.B. Duke, in *Surface Properties of Electronic Materials*, edited by D.A. King and D.P. Woodruff (Elsevier, Amsterdam, 1988), pp. 69–118.

[11] J.P. LaFemina, Surf. Sci. Rep. **16**, 133 (1992).